

# Complete T<sub>1</sub>, T<sub>2</sub>\* and Proton-Density Maps of Bone and Soft Tissues from UTE and Standard FLASH

Jean-David Jutras<sup>1</sup>, Keith Wachowicz<sup>1,2</sup>, B. Gino Fallone<sup>1,2</sup>, and Nicola DeZanche<sup>1,2</sup>

<sup>1</sup>Dept. of Oncology, University of Alberta, Edmonton, Alberta, Canada, <sup>2</sup>Dept. of Medical Physics, Cross Cancer Institute, Edmonton, Alberta, Canada

## Purpose

Achieving optimal bone and soft-tissue contrast simultaneously with a single imaging modality is challenging. The traditional solution consists of co-registering a CT dataset with a MRI dataset, providing both the bone information from CT and soft-tissue contrast from MRI. The use of ultra-short echo time (UTE) MRI permits the visualization of bone, but at the cost of low signal-to-noise ratio (SNR) in soft-tissues and long scan times compared to standard Cartesian MRI [1]. In this phantom study, we propose segmenting and fusing bone and soft-tissue T<sub>1</sub>, T<sub>2</sub>\* and proton-density (PD) information from two types of MRI scans (UTE and standard FLASH) as an MRI-only alternative to MRI-CT fusion.

## Theory

Driven Equilibrium Single Pulse Observation (DESPOT) performs fast 3D T<sub>1</sub> mapping by employing FLASH datasets at two or more flip angles "tuned" to achieve optimal T<sub>1</sub>-to-noise ratio, while keeping all other parameters the same [2]. Assuming perfect spoiling, the FLASH signal is given by

$$M_{xy} = \frac{M_0 f_{xy} (1 - E_1)}{1 - f_z E_1} e^{-TE/T_2^*}, \quad (1)$$

where  $E_1 = \exp(-TR/T_1)$ . For the soft-tissue signal,  $f_{xy} = \sin(\alpha)$  and  $f_z = \cos(\alpha)$ , while for the bone signal an alternate analytical expression exists, which takes the effect of T<sub>2</sub>\* decay during the RF excitation pulse [3]. Equation (1) is linearized to reduce post-processing time. We found it sufficient to use the same  $f_{xy}$  and  $f_z$  also for bone as long as its T<sub>1</sub> is converted to a true T<sub>1</sub> by a correction factor estimated from the exact analytical expression. Using a double-echo UTE FLASH sequence at two tuned flip angles, the T<sub>1</sub>, T<sub>2</sub>\* and PD of bone can all be obtained from Eq.(1). Similarly, the same quantitative information may be obtained for soft-tissues using multi-echo Cartesian FLASH.

## Methods

A bone, petroleum jelly and agar phantom was prepared to test the proposed technique. Bovine femur cortical bone was cleaned and filled with petroleum jelly to mimic bone marrow. Three different layers of agar doped with MnCl<sub>2</sub> were poured in the phantom (separated by cellophane wrap to prevent diffusion), providing T<sub>1</sub> and T<sub>2</sub> values in the range of soft-tissues. The phantom was scanned on a 3T Philips Achieva MRI scanner, with a 8-channel head array coil with a resolution of 1x1x2 mm<sup>3</sup> (70 sagittal slices) and a field-of-view (FOV) of 220x220x140 mm<sup>3</sup>. The following DESPOT protocols with non-selective RF excitation were used: a) 3D UTE FLASH,  $\alpha_1/\alpha_2=33/6^\circ$ , TR=7.2 ms, T<sub>E1</sub>/T<sub>E2</sub>=0.09/1.8 ms, BW=388 kHz, 25270 spokes, 6:00 min; b) standard 3D Cartesian 7-echo FLASH with  $\alpha_1/\alpha_2=20/4^\circ$ , TR=16 ms, TE<sub>1</sub>/ΔTE=1.9/2.1 ms, BW=265 kHz, 6:30 min. Correction for flip-angle non-uniformity was performed in soft tissues using a dual-TR B<sub>1</sub><sup>+</sup>-mapping protocol: 3.4x3.5x4 mm<sup>3</sup> resolution, 35 sagittal slices, T<sub>E</sub>=1.28 ms, TR<sub>1</sub>/TR<sub>2</sub>=20/100 ms, α=60°, 3:18 min [4]. The bone T<sub>1</sub>, T<sub>2</sub>\* and PD were calculated and segmented from the UTE datasets and pasted into the corresponding areas of the soft-tissue maps derived from the standard FLASH datasets. Segmentation was performed using a method similar to Ref. [5], except that thresholding was done on T<sub>1</sub> and T<sub>2</sub>\* simultaneously for improved accuracy. A 2D IR-GraSE scan (T<sub>1</sub>=50, 250, 500, 800, 1200, 1700 and 2400 ms, T<sub>E</sub>/T<sub>R</sub>=12 ms/10 s, TSE factor=5, EPI factor=5, 1x1x6 mm<sup>3</sup> resolution) was used as a standard for comparison of the soft-tissue T<sub>1</sub> values (Fig. 1b) by curve-fitting to  $M_z = M_0(1-\beta)e^{-T_1/T_1}$ , where β accounts for imperfect inversion.

## Results

As shown in Fig. 1 (a-c), there is good agreement between the T<sub>1</sub> values of IR compared to DESPOT where the B<sub>1</sub><sup>+</sup> correction is accurate. Some systematic errors tend to occur at the edges of the bone likely due to B<sub>1</sub><sup>+</sup> inaccuracy, and at tissue boundaries due to distortions in the IR-based images. As expected, IR-GraSE could not accurately measure the T<sub>1</sub> of bone or petroleum jelly due to the very short T<sub>2</sub>\*. The final combined T<sub>1</sub> map is displayed in Fig. 2. The peak of the bone T<sub>1</sub> histogram occurred at ~170ms, and the T<sub>2</sub>\* at ~0.75ms. Noise addition from the multi-channel image combination pushes the T<sub>2</sub>\* to an apparent value longer by ~0.25ms than the expected ~0.5ms, assuming a mono-exponential decay [1, 6]. The peak T<sub>1</sub> of petroleum jelly occurred at ~205ms, with T<sub>2</sub>\* at ~8.3ms.

## Conclusion

Our proposed technique provides three different contrast mechanisms and high SNR in all tissue types through the segmentation and combination of radial UTE and Cartesian FLASH quantitative MRI information in about 16 min of total scan time. Potential applications of the technique include radiation therapy treatment planning, linear attenuation corrections with bone and soft-tissue contrast in PET-MRI, the diagnosis and monitoring of bone cancer, and image-guided surgery.

**Acknowledgements:** The authors wish to acknowledge funding from the Alberta Cancer Foundation.

**References:** [1] M. D. Robson et al. J Comput Assist Tomogr 27:825-846 (2003). [2] S. C. L. Deoni et al. Magn Reson Med 49:515-526 (2003). [3] M.S.Sussmann et al. Magn Reson Med 40: 890-899 (1998). [4] V. L. Yarnyck. Magn Reson Med 57:192-200 (2007). [5] V. Keereman et al. J Nucl Med 51:812-818 (2010). [6] P. A. Hardy et al. Magn Reson Med 61:962-969 (2009).

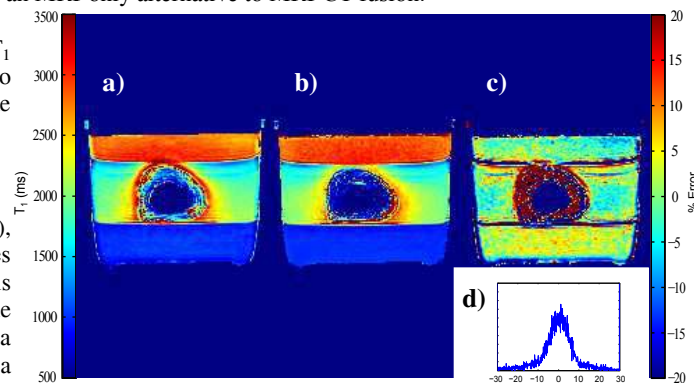


**Figure 1:** (a) T<sub>1</sub> map derived from Cartesian DESPOT only. (b) T<sub>1</sub> map derived from IR-GraSE. (c) Percent error (DESPOT-IR)/IR×100%. (d) Histogram of the percent error.

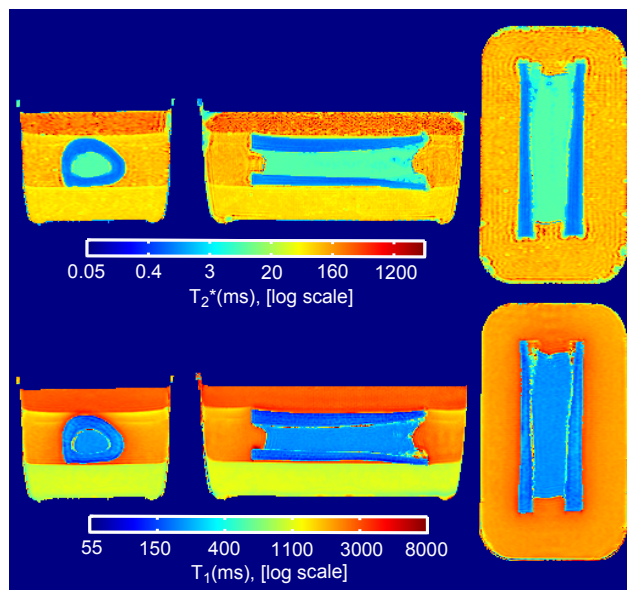


**Figure 2:** Complete T<sub>1</sub> and T<sub>2</sub>\* maps (note logarithmic scales) derived from both the UTE and Cartesian FLASH datasets.